PAPER • OPEN ACCESS

^{68}Ga-adsorption on the Si-nanoparticles

View the article online for updates and enhancements.

IOP ebooks™

Bringing you innovative digital publishing with leading voices to create your essential collection of books in STEM research.

Start exploring the collection - download the first chapter of every title for free.

^{68}Ga-adsorption on the Si-nanoparticles

H S Skrabkova[1,3], V B Bubenschikov[2], G E Kodina[2], A S Lunev[2], A A Larenkov[2], N B Epshtein[3] and A V Kabashin[4]

[1]Chemistry Department, Belarusian State University, Minsk 375-17-226-59-40, Republic of Belarus

[2]Burnasyan Federal Medical Biophysical Center, Moscow, Russia

[3] Obninsk Institute for Nuclear Power Engineering National Research Nuclear University MEPhI, Obninsk, Russia

[4]Aix-Marseille University, Marseille Cedex 9, France

E-mail: skrebkova.a@gmail.com bubenschikov2011@yandex.ru gkodina@yandex.ru

Abstract. In recent years, more and more attention has been paid to nanoparticles (NPs) as target drug delivery systems. Silicon-based nanoparticles are one of the most biocompatible nanomaterials that have become widespread. In this research, we studied the possibility of gallium-68 sorption on silicon (Si-SiO$_x$) and silicon dioxide (SiO$_2$) nanoparticles without their surface modification. Conditions allowing to obtain ^{68}Ga-NPs with radiochemical yield $\geq 90\%$ were found. ^{68}Ga-SiO$_2$ showed much higher stability over ^{68}Ga-Si-SiO$_x$ in both *in vitro* and *in vivo* experiments.

1. Introduction

Nanoparticles (NPs) for biomedical applications have become very popular field of research in the last few decades. Every year the number of papers on this subject increases significantly due to the development of new methods of synthesis of nanomaterials and nanocomposites. Among the large number of nanomaterials, special attention is paid to the NPs of silicon and silicon dioxide. This is due to the fact that they have features such as monodispersity, large surface area, the possibility of high-performance loading of drugs. In addition, their surface can be modified with target ligands or chelating agents [1]. Compared to other nanomaterials, silicon dioxide NPs are biocompatible [2], resistant range to temperature, mechanical stress, and degradation caused by hydrolysis in a wide pH [3]. Thus, silicon dioxide NPs are one of the most frequently used materials in biomedical research [4]. Possibility of their uses, as systems for the delivery of drugs [5], gene transfection [5], contrast agents [6], solutions for radionuclide diagnosis and treatment of tumors [7] has been actively studied in the world. In addition to biomedical applications, silicon dioxide is used in analytical chemistry to separate elements as a stationary phase in chromatographic analysis.

However, one of the problems of SiO$_2$ nanoparticles is the fact that they are not biodegradable and accumulate in various organs, especially in the kidneys and liver, which causes many negative effects. Silicon NPs obtained by laser ablation are Si nanocrystals coated with a thin layer of silicon oxide (Si-SiO$_x$) [8]. These NPs are biodegradable and considered as a perspective framework for the creation of various drugs [9].

Labeled NPs can be used for lymphoscintigraphy, particularly for intraoperative imaging of sentinel lymph nodes (SLN) [10]. Nanocolloid, labeled with ^{99m}Tc, is a perfect product for identifying the SLN, however, the search for other radiopharmaceuticals is still in progress all over the world [11].

In addition, available radiopharmaceuticals contain only ^{99m}Tc, which is used exclusively for the visualization with single photon emission computed tomography. From this perspective the development of other similar radiopharmaceuticals for positron emission tomography (PET) is required.

^{68}Ga is one of the most perspective radionuclides for the development of radiopharmaceuticals for PET. It is related to fact that ^{68}Ga is a generator radionuclide and has optimal nuclear physical characteristics. Gallium-68 decays with the emission of positrons (89%) and by electronic capture (EZ, 11%). The average energy of positrons per decay is 740 keV ($E_{\beta}^{+}{}_{max}$ = 1899 keV) [12]. The half-life is 67.71 minutes. The decay is accompanied by the emission of annihilation γ-quants ($E_{\gamma 1}$ = 511 keV, yield 180 %; $E_{\gamma 2}$ = 1077 keV, yield 2,93 %) [13], figure 1.
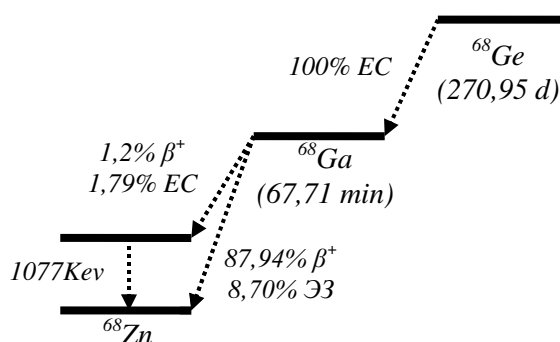

Figure 1. ^{68}Ge decay scheme.

Nowadays, a large number of studies of radioisotope binding to the surface of various NPs, including silicon dioxide, are well known. However, the main part of these studies is based on the modified surface of NPs, whereby the binding of radioisotopes to the surface of NPs occurs through molecular chelating agents [14], whereas the direct adsorption of radioisotopes on NPs is poorly studied [1]. Therefore, the aim of this work was to study the possibility of gallium-68 adsorption on silicon dioxide NPs without modifying the surface.

2. Materials and methods
^{68}Ga was obtained from ^{68}Ge/^{68}Ga generator ('Cyclotron Co., Ltd.', Obninsk, Russia). The radioactivity was measured with 'Atomlab 500' dose-calibrator (Biodex Medical Systems, Inc., USA). All the experiments were performed using deionized water (18 MOm•cm).

All reagents used in the work belonged to the class of pure ones, particularly: sodium acetate (Macco Organiques, Czech Republic), sodium tartrate (Alfa Aesar, USA), sodium succinate (Sigma-Aldrich), sodium trifluoroacetate (Sigma-Aldrich), sodium phosphate (Panreac, Spain), HEPES (Panreac, Spain), sodium carbonate, sodium hydroxide, hydrochloric acid 0.1 M (Panreac, Spain), ammonium acetate (Panreac, Spain).

Two types of NPs were used: silicon dioxide of 10-20 nm particle size by Sigma-Aldrich (SiO_2) and silicon NPs covered with a layer of silicon oxide of 50 nm particle size (Si-SiO_x). In experiments on the order of mixing of the reagents two types of SiO_2 NPs were used: 10-20 nm sized NPs by Sigma-Aldrich and 100 nm sized NPs 'Polisorb MP'.

Radiolabeling procedure was performed as follows. A buffer solution and suspension containing NPs were placed into an Eppendorf tube followed by adding of the eluate of the ^{68}Ge/^{68}Ga generator. The concentration of NPs in the samples was 5-70 µg/mL. The tubes were incubated in for 15, 30 and

60 minutes at 25, 70 and 95 °C. A control sample (without NP) was prepared and analyzed in parallel with every sample. Radiochemical yield was controlled with radiometry and TLC.

Radiometry was carried out as follows. 10 µL aliquot of every sample was taken immediately after the end of labeling process. Then samples containing NPs were centrifuged for 1-10 minutes at 15k rpm. 10 µL aliquot of supernatant of every sample was taken after centrifugation. The amount of adsorbed ^{68}Ga was determined by the formula:

$$A_{\mathrm{r}} = \left(1 - \frac{A_l}{A_g}\right) \cdot 100\% = \frac{A_g - A_l}{A_g} \cdot 100\%$$

where A_{r} – sediment radioactivity related to the total activity; A_g – of the sample taken before the centrifugation; A_l – radioactivity of the sample taken after the centrifugation.

TLC was performed on ITLC-SG strips (Agilent Technologies, USA). Aqueous solution of citric acid (0.05 M), aqueous solution of sodium citrate (0.1 M, pH 4.6), 4% trifluoroacetic acid (TFA) were used as eluents. In all systems, the free ^{68}Ga advances with the solvent front, while the hydrolyzed and associated ^{68}Ga NPs remain at the origin: $R_{f\ ^{68}Ga-free} = 0{,}8 - 1{,}0$; $R_{f\ ^{68}Ga-associated\ with\ nanoparticles} = 0 - 0{,}2$; $R_{f\ ^{68}Ga-colloid} = 0 - 0{,}2$. The radioactivity distribution along the chromatographic strip was evaluated using 'miniGita Star' scanner for thin-layer chromatography ('Raytest', Germany).

In vivo experiments were carried out on BALB/C mice. The radiopharmaceutical was administered to laboratory animals intravenously into the tail vein in the amount of 0.1 ml with radioactivity of no more than 20 MBq/ml. The biodegradable was visualized with PET/X-RAY Genisys4 positron emission tomograph for laboratory animals (SofieBioscience, USA). The scanning procedure was performed 60 minutes after intravenous injection. The scanning time was 10 minutes.

3. Results

3.1. System selection for TLC

Similarly to the methods described in [1], to estimate the adsorption of ^{68}Ga on the surface of NPs we tried different stationary phases (ITLC-SG, Silica gel 60, TLC Cellulose F, Whatman-2) with different eluents (aqueous solutions of citric acid, sodium citrate, sodium acetate, EDTA, DTPA, TFA; mixture of acetonitrile and water, etc.). Three chromatographic systems were chosen: aqueous solution of citric acid, aqueous solution of sodium citrate and 4% (TFA) on ITLC-SG strips. However, when comparing chromatograms of sample with NPs and corresponding control sample, it was noted that the radioactivity at the origin of chromatographic plates for control samples was higher than for analogous samples with silicon dioxide NPs. It can be assumed that when mixing components, gallium is sorbed onto the surface of NPs before the maximum formation of its hydroxyl forms occurs, that is, gallium adsorption takes place in all its forms: Ga^{3+}, $Ga(OH)^{2+}$, $Ga(OH)_2^{+}$, $Ga(OH)_3$, while in control sample gallium is maximally hydrolyzed to form $Ga(OH)_3$. Therefore, it can be assumed that gallium sorbed on silicon dioxide nanoparticles in ionic forms is desorbed by these eluents.

Also, in these systems, a significant discrepancy was found in the evaluation of ^{68}Ga adsorption on the surface of silicon dioxide NPs by TLC and radiometry. According to the results of radiometry, radioactivity was concentrated on nanoparticles, while according to TLC the amount of ^{68}Ga-NPs was significantly lower. The difference in the results between TLC and radiometry can be explained by the fact that the eluting solvent is sufficient to partially desorb gallium from the surface of the nanoparticles. It can be concluded that ionic ^{68}Ga is weakly retained on the surface of nanoparticles and transchelated by the eluent. Mostly the results of radiometry were used to estimate the adsorption.

3.2. Effect of pH on adsorption ^{68}Ga on NPs

In the view of the configurational lability of gallium [15], one of the key parameters is the pH of the system. We began to study the adsorption of ^{68}Ga from experiments in various pH ranges. We observed adsorption in excess of 90% in the pH range from 4.0 to 6.5 in the presence of sodium acetate, as a buffer agent (figure 2). At such pH values, gallium is presented   in   hydrolyzed   forms:
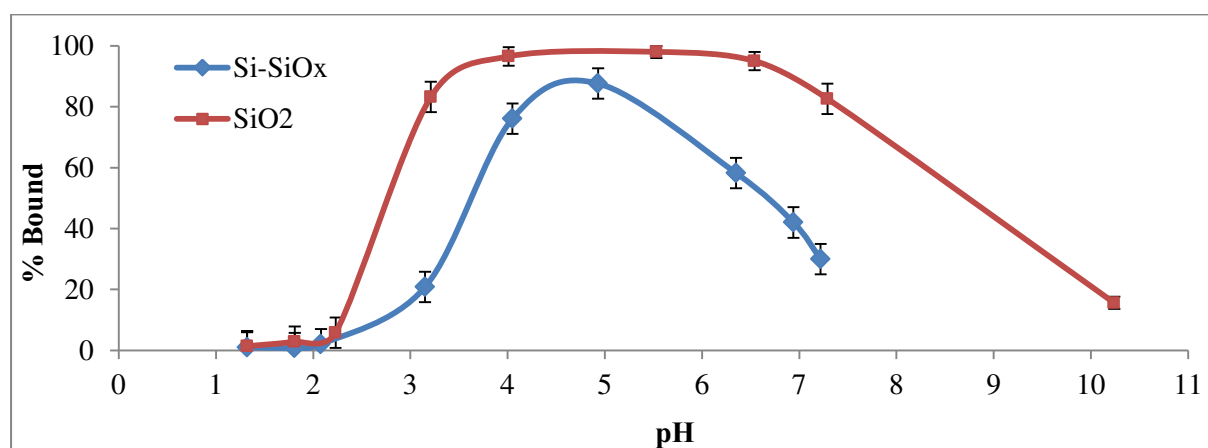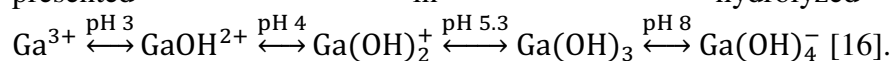
$$Ga^{3+} \xoverset{pH\ 3}{\longleftrightarrow} GaOH^{2+} \xoverset{pH\ 4}{\longleftrightarrow} Ga(OH)_2^+ \xoverset{pH\ 5.3}{\longleftrightarrow} Ga(OH)_3 \xoverset{pH\ 8}{\longleftrightarrow} Ga(OH)_4^- \text{ [16].}$$

Figure 2. Plot of the percentage of ^{68}Ga bound to particles surface versus reaction pH; incubation 30 min, 70 °C.

The silanol groups on the surface are involved in the adsorption process. Thus, the charge of hydrolyzed forms of gallium, as well as the number of hydroxyl groups, affects gallium adsorption on silicon dioxide nanoparticles. Consequently, it can be assumed that the adsorption is due to the formation of hydrogen bonds of oxygen atoms of hydrolyzed gallium forms with OH groups on the surface of silicon dioxide.

It should be noted that effective adsorption was observed only with the use of sodium acetate, with the maximum adsorption being observed in the pH range of 4.0-6.5 and accompanied by coagulation.

The use of stabilizer (TWEEN 80) positively affected the aggregative stability but led to a drop in adsorption (figure 3).
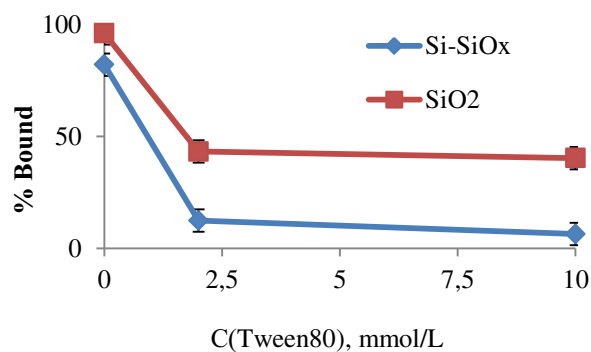

Figure 3 Plot of the percentage of ^{68}Ga bound to particles surface versus concentration of TWEEN 80, pH 4.1, 30 minutes, 70 °C.

3.3. The study of adsorption of ^{68}Ga colloid forms on NPs

To select the system in which maximum formation of the ^{68}Ga-colloid will occur, reaction mixtures in the pH range from 3 to 7 in the presence of various buffer agents (sodium acetate, sodium phosphate, sodium carbonate, sodium succinate, HEPES, ammonium acetate) were considered. The highest yield of ^{68}Ga-colloid was observed in reaction mixtures with ammonium acetate and sodium carbonate at pH 5. These systems were chosen for further investigation of adsorption of ^{68}Ga on SiO$_2$-NPs. During the experiments, it was noted that the order of mixing of the reagents affects the adsorption of ^{68}Ga on nanoparticles. Two orders of mixing of reagents were studied:

I. ^{68}Ga eluate was added to the NPs solution, followed by a buffer solution. The sample was incubated for 15 minutes at room temperature.

II. ^{68}Ga eluate was added to the solution of the buffering agent and incubated for 15 minutes at room temperature to form colloid, after which solution of silica nanoparticles was added and again incubated for 15 minutes at room temperature.

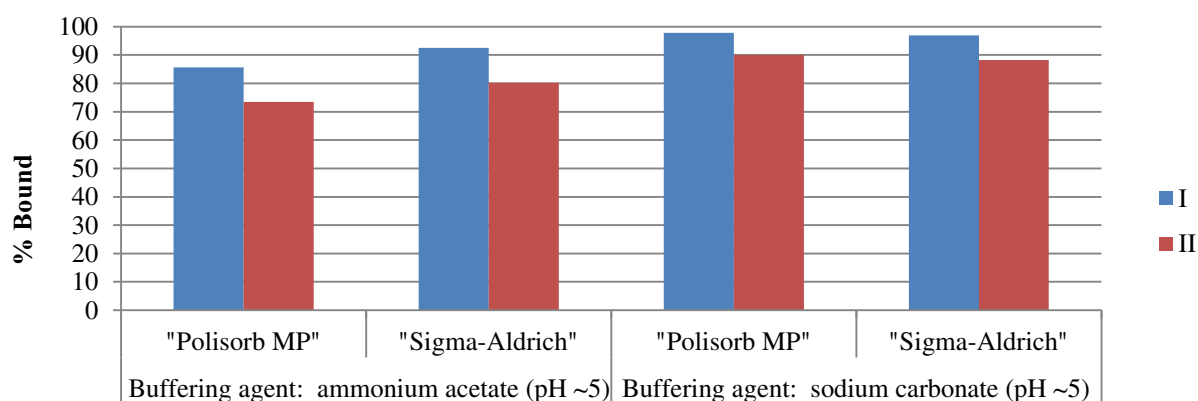The results of the experiment are shown in figure 4.

Figure 4. Plot of the percentage of ^{68}Ga bound to particles surface versus the order of mixing of the reagents.

When the order of mixing from I to II is changed, ^{68}Ga adsorption on nanoparticles decreases, the data is consistent for two types of silicon dioxide nanoparticles, as well as using different buffering agents. It can be assumed that with the order of mixing of reagents, several independent processes occur in the system: the formation of ^{68}Ga-colloid and its adsorption on the surface of nanoparticles, as well as adsorption of partially hydrolyzed forms of ^{68}Ga and hydrated ionic forms of ^{68}Ga. Moreover, in the first order of mixing the reagents on the nanoparticle surface, it is the ionic forms of ^{68}Ga that are immediately adsorbed, since the nanoparticle solution immediately mixes with the eluate, and only then is a solution of the buffering agent added that affects the formation of the ^{68}Ga-colloid. From this it can be concluded that the best adsorption of ^{68}Ga on the surface of nanoparticles occurs during the course of competitive processes, namely adsorption of colloidal and ionic forms of ^{68}Ga.

3.4. Comparison of SiO$_2$ NPs with Si-SiO$_x$ NPs

Further, we carried out comparative experiments on the adsorption of ^{68}Ga on SiO$_2$, Si-SiO$_x$ nanoparticles. The experiments were performed at pH 7.3, since nanoparticles exhibit high aggregative stability at pH > 7. The results are shown in figure 5–7.

The obtained data allow us to conclude that with an increase in temperature to 95°C there is a decrease in adsorption of ^{68}Ga on SiO$_2$ nanoparticles.

Despite the rather low ^{68}Ga adsorption results on Si-SiO$_x$ nanoparticles at pH 7.3, it was decided to carry out a biological study with both SiO$_2$, Si-SiO$_x$ nanoparticles. Nanoparticles labeled with ^{68}Ga (amount of SiO$_2$ = 0.625 mg/kg of body weight; amount of Si-SiO$_x$ = 0.22 μg/kg of body weight; 2

MBq per mice) were injected to BALB/c mice in the tail vein. 60 minutes after the injection PET images were obtained ('PET/X-RAY Genisys4', Sofie Bioscience, USA). The results of the imaging are presented in figure 8.

Labeled nanoparticles SiO_2 accumulate only in the liver and are not excreted in the urine within 60 minutes after the injection, while the free ^{68}Ga remains in the blood. This is evidenced by a strong contrast on the images obtained (figure 9a). It should be noted that $Si-SiO_x$ nanoparticles have significant background accumulation in the bloodstream and bladder (figure 9b), which indicates a large amount of free ^{68}Ga. According to our data, the low thickness of the oxide layer and the lack of a developed surface is the main problem for successful labeling.
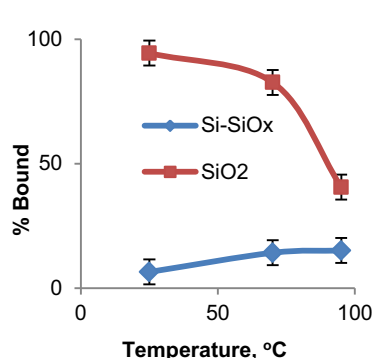

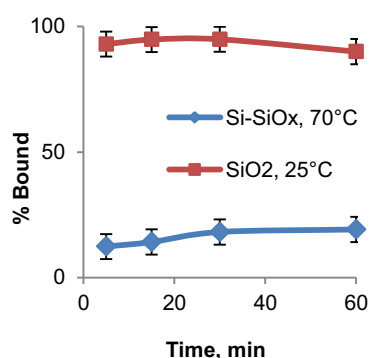**Figure 5.** Plot of the percentage of ^{68}Ga bound to particles surface versus reaction temperature, pH 7.3; 30 min.

Figure 6. Plot of the percentage of ^{68}Ga bound to particles surface versus reaction time, pH 7.3; 70 °C.
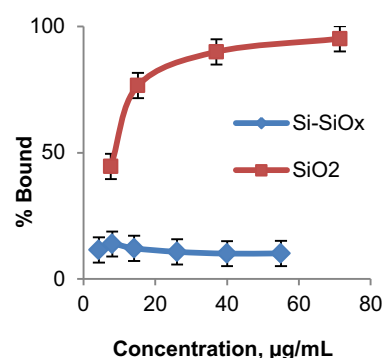
Figure 7. Plot of the percentage of ^{68}Ga bound to particles surface versus concentration of nanoparticles.
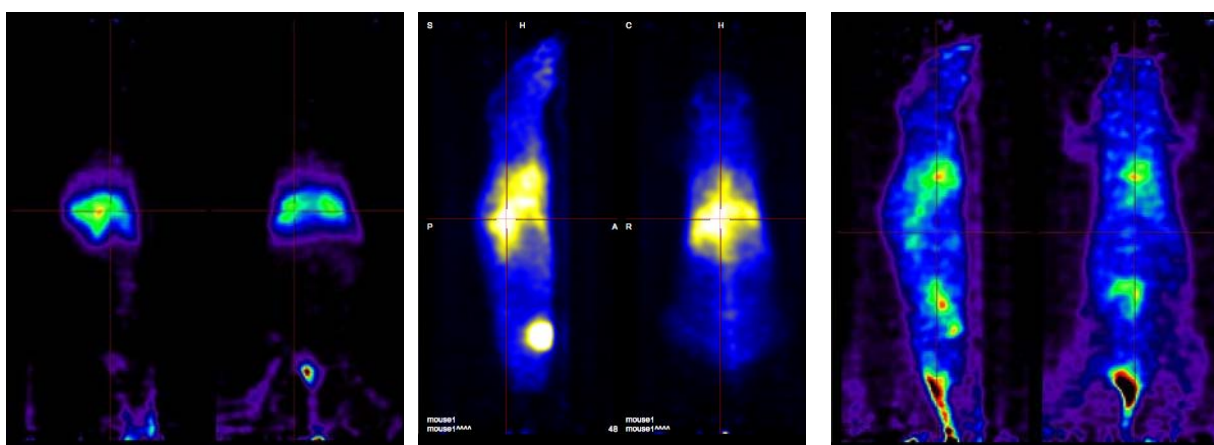

Figure 8. In vivo PET imaging (a) $^{68}Ga-SiO_2$; (B) $^{68}Ga-Si-SiO_x$; (C) free ^{68}Ga.

4. Conclusion

As a result of the study, we conclude that ^{68}Ga is better adsorbed on SiO_2 nanoparticles than on $Si-SiO_x$. ^{68}Ga adsorption on $Si-SiO_x$ nanoparticles occurs in lower quantities and only when accompanied by coagulation, this is due to the low thickness of the oxide layer and the lack of a developed surface in $Si-SiO_x$ nanoparticles. The use of the stabilizer has a positive effect on aggregate stability, but leads to a drop in adsorption. With the increase in temperature to 95°C, ^{68}Ga sorption on SiO_2 nanoparticles

decreases, this decline is associated with an increase in the degree of hydrolysis of ^{68}Ga and the formation of a large number of colloidal forms. Obtained data and the results of *in vivo* experiments indicate the possibility of sorption of ^{68}Ga on the surface of SiO$_2$ and Si-SiO$_x$ nanoparticles without surface modification.

References
[1]   Shaffer T M, Wall M A, Harmsen S, Longo V A, Drain, C M, Kircher M F and Grimm J 2015 *Nano Lett.* **15** 864–8
[2]   Slowing I I, Wu C W, Vivero-Escoto J L and Lin V S 2008 *Adv. Drug. Deliv. Rev.* **60** 1278–88
[3]   Kretowski R, Kusaczuk M, Naumowicz M, Kotynska J, Szynaka B and Cechowska-Pasko M 2017 *Nanomaterials (Basel).* **7** 230
[4]   Zhou Y, Quan G, Wu Q, Zhang X, Niu B, Wu B, Huang Y, Pan X and Wu C 2018 *Acta Pharm. Sinica. B.* **8** 165–77
[5]   Chen M and von Mikecz A 2005 *Exp. Cell. Res.* **305** 51–62
[6]   Bradbury M S, Pauliah M, Zanzonico P, Wiesner U and Patel S 2016 *Wiley Interdiscip. Rev. Nanomed. Nanobiotechnol.* **8** 535–53
[7]   Barrett T, Choyke P L and Kobayashi H 2006 *Contrast. Media. Mol. Imaging.* **1** 230–45
[8]   Gongalsky M B et al. 2016 *Sci. Rep.* **6** 24732
[9]   Baati T et al. 2016 *Sci. Rep.* **6** 25400
[10] Vera D R, Wallace A M, Hoh C K and Mattrey R F 2001 *J. Nucl. Med.* **42** 951–9
[11] Hodgson N, Zabel P, Mattar A G, Engel C J, Girvan D and Holliday R 2001 *Ann. Surg. Oncol.* **8** 133–7
[12] Fani M, Andre J P and Maecke H R 2008 *Contrast. Media. Mol. Imaging.* **3** 67–77
[13] Saha Gopal B 2010 *Fyndamentals of Nuclear Pharmacy* (New York: Springer) p 79
[14] Xing Y, Zhao J, Conti P S and Chen K 2014 *Theranostics* **4** 290–306
[15] Taylor M J 1990 *Polyhedron* **9.2-3** 207–14
[16] Wood S A and Samson I M 2006 *Ore Geology Reviews* **28** 57–102